

Modeling Dissolved Oxygen in a Dredged Lake Erie Tributary

Jagjit Kaur^{1,†}, Gopi Jaligama², Joseph F. Atkinson³, Joseph V. DePinto^{4,*},
and Adrienne D. Nemura⁴

¹CH2M HILL

1000 Wilshire Boulevard, 21st Floor
Los Angeles, California 90017

²TRC Omni Environmental Corporation
Research Park, 321 Wall Street
Princeton, New Jersey 08536

³University at Buffalo
Buffalo, New York 14260

⁴Limno-Tech, Inc.
501 Avis Drive
Ann Arbor, Michigan 48108

ABSTRACT. A two-dimensional numerical model was developed to study dissolved oxygen (DO) kinetics in a dredged Lake Erie tributary. The model design was aimed to specifically address the fact that many tributaries to the Great Lakes are dredged periodically for navigation, and that resultant changes in morphology and hydraulics can have significant impacts on DO. Due to the greater depths caused by dredging, river velocities slow considerably and vertical mixing is not as effective, leading to thermal stratification and potential short-circuiting of warmer upstream flow. The model solves the two-dimensional (laterally averaged) hydrodynamic and mass balance equations to simulate transport and transformation relevant to dissolved oxygen using an alternating direction, implicit finite difference method. Effects of oxygen-demanding pollutants from municipal and industrial discharges and also from nonpoint sources are included. A model application was developed for the Black River (Ohio), a tributary of Lake Erie. The river is dredged periodically, becomes stratified during the low flow summer months, and is affected by changing lake levels associated with seiching in Lake Erie. After calibration and confirmation, the model was used as a diagnostic tool to understand the impact of various loading sources on low DO levels observed along the bottom of the river. It is shown that sediment oxygen demand (SOD), combined with the river hydraulics, is the primary cause for low DO levels in the Black River.

INDEX WORDS: Dissolved oxygen, Great Lakes tributaries, sediment oxygen demand, modeling.

INTRODUCTION

Many tributaries in the Great Lakes are dredged for navigational purposes. Dredging usually involves the periodic removal of accumulated bottom sediments from waterways to enlarge or deepen a navigation channel. The resultant changes in morphology and hydraulics can have significant impacts on water quality. Dissolved oxygen (DO) is one of the most important variables in water quality analysis, and many of these tributaries suffer from low DO con-

centrations, particularly in the summer months. Low DO concentrations directly affect fish and alter a healthy ecological balance. Because DO is affected by many other water quality parameters, it is a sensitive indicator of the health of an aquatic system. To protect warm water fish and plant life, many water quality standards require that DO be greater than 4 milligrams per liter (mg L^{-1}), with a daily minimum average of 5 mg L^{-1} , and temperatures must be less than maximum criteria, which vary depending on the time of the year (U.S. EPA 1986).

When coupled with large swings in surface ele-

*Corresponding author. E-mail: jdepinto@limno.com

† formerly with Limno-Tech, Inc.

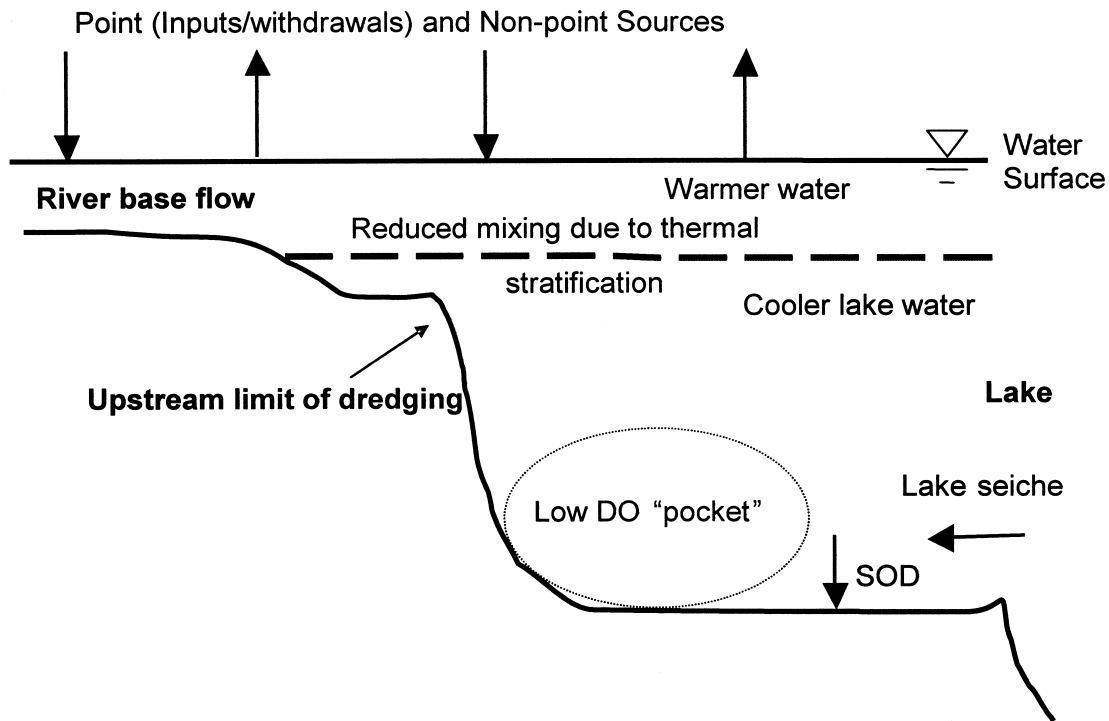


FIG. 1. Conceptualization of conditions in the dredged Great Lakes tributaries (see text for details).

vation of the lake into which it discharges, dredged tributaries can behave like estuaries, with frequent and significant flow reversals and rapid changes in water levels. The dredged portions have depths that may be four to six times the normal depth of the river and are characterized by low velocities and decreased vertical mixing. The differences in temperatures and densities between the river and lake waters in the warmer summer months lead to vertical stratification and potential short-circuiting of upstream flow, where the warmer river flow remains at the surface. Stratification reduces vertical mixing, which reduces the downward transfer of surface oxygen, and sediments exert oxygen demand, resulting in low DO concentrations in the bottom waters. A conceptual sketch of conditions affecting DO concentrations in a dredged tributary is depicted in Figure 1. Discharges from point sources, such as industries, wastewater treatment plants, sanitary sewer overflows (SSOs) and combined sewer overflows (CSOs), and nonpoint sources (surface runoff) also contribute to low DO concentrations in the receiving waters. To understand the DO problems occurring in these tributaries, the spatial resolution needed for any hydrodynamic/water quality model must incorpo-

rate at least a two-dimensional (laterally averaged) structure. On the other hand, data availability is usually such that a fully three-dimensional approach is not warranted. The present model adopts a two-dimensional framework.

A number of existing water quality models, such as WASP (Wool *et al.* 2003), QUAL2E (Brown and Barnwell 1987), and CE-QUAL-W2 (Cole and Buchak 1995) simulate DO transport in rivers, but those models are not directly applicable for evaluating DO kinetics in the dredged portions of rivers. For example, the WASP (which uses DYNHYD, a one-dimensional hydrodynamic model) and QUAL2E models simulate only longitudinal velocity profiles, whereas CE-QUAL-W2, a two-dimensional, longitudinal/vertical, hydrodynamic and water quality model, was found to require a large number of inputs and modifications to the source code in order to adequately represent conditions for dredged tributaries of the Great Lakes. Moreover, CE-QUAL-W2 uses a z-grid computational approach. Terrain following models tend to be more stable than the z-grid models and have distinct advantages in terms of specifying the bottom boundary conditions. It is important to build a modeling framework capable of describing the longitudinal gradients as well as vertical stratifi-

cation, which is essential for simulating conditions in dredged channels and to evaluate the impacts of oxygen-demanding pollutants on DO. In addition, other requirements of the model include the ability to handle multiple point and nonpoint sources to account for time-varying discharges, withdrawals from various sources, watershed runoff, impacts of the lake seiche, and time-dependent boundary conditions.

The specific goal of this study was to develop a coupled two-dimensional, laterally averaged, hydrodynamic and water quality model that could be used to evaluate the impacts of oxygen demanding sources and assess the factors contributing to low DO in the dredged portions of Great Lakes tributaries. The model was built upon a previously developed framework (Blair 1992, Wight 1995, Hall 1997), which was originally designed to evaluate sources of oxygen demand in the Buffalo River, Buffalo, New York. In the present study the model is applied to the Black River, which enters Lake Erie at Lorain, Ohio.

The model application was conducted to determine the feasibility of meeting warm water DO standards. Specifically, the model was designed to understand the impact of various point and non-point sources of pollutants along with changes in morphology and hydraulics caused by navigational dredging on DO dynamics. Numerical experiments were conducted to test the hypothesis that SOD, coupled with the altered system hydraulics, is the primary cause of low DO levels in the bottom waters of the dredged tributary. Diagnostic and sensitivity analyses were conducted to understand the mechanisms affecting the low DO concentrations.

MODEL DEVELOPMENT

Conceptual Model Approach

The overall modeling approach used in this study involved coupling of a two-dimensional, laterally averaged, hydrodynamic model and a water quality model. The hydrodynamic model is based on continuity and momentum balances. Hydrodynamic constituents include water depth and vertical and horizontal velocities. The water quality model calculates values for water quality constituents using basic mass balances, as expressed through the advection-diffusion equation, while incorporating appropriate sources and sinks. Water quality constituents include temperature, carbonaceous biochemical oxygen demand (CBOD), ammonia (NH_3), nitrate (modeled as nitrate plus nitrite,

NO_3+NO_2), total organic nitrogen (TON), and dissolved oxygen (DO). The water quality model contains an SOD formulation that allows spatially variable SOD rates to change with temperature and water column DO.

The numerical discretization is a terrain-following coordinate system, with an equal number of layers (referred to as "sigma layers") everywhere in the model domain. In other words, the layer thickness expands in deeper portions of the river and becomes thinner in shallower regions. This type of formulation simplifies the finite difference representation for the system, but may produce errors when flows are very high or when there are rapid changes in depth. To avoid these problems, care must be taken to choose a combination of longitudinal grid length, number of layers, and time step. In addition to sigma layers, a staggered grid approach is adopted in which velocities are defined at the edges of the grid, while the concentrations of nutrients, temperature, density and viscosity of water are defined at the center of the grid as shown in Figure 2. This method is numerically stable and effective in limiting excessive computational time associated with solving the non-linear momentum equation (Kantha and Clayson 1994). The model is formulated to handle up to 20 layers in the vertical direction and up to 200 grids (or segments) longitudinally.

The alternating direction implicit (ADI) method (Zhao 2002) was used to solve the governing equation in two steps. In the first half time step, consecutive layers of elements are solved implicitly by holding adjacent elements, above and below, as constant at their values from the previous time step. In the second half time step, a similar procedure is followed, solving consecutive columns along the model reach. All concentration values are updated only after one full sweep is completed. A derivation of the general finite difference expressions for the two-dimensional advection diffusion equation is presented by Jaligama (2004).

Hydrodynamic Model

The hydrodynamic model uses the momentum equation to solve for longitudinal velocities (Clark 1996),

$$\frac{\partial UW}{\partial t} + U \frac{\partial UW}{\partial x} + V \frac{\partial UW}{\partial z} = -\frac{W \nabla P}{\rho} + \frac{\partial}{\partial x} \left(v_x \frac{\partial UW}{\partial x} \right) + \frac{\partial}{\partial z} \left(v_z \frac{\partial UW}{\partial z} \right) \quad (1)$$

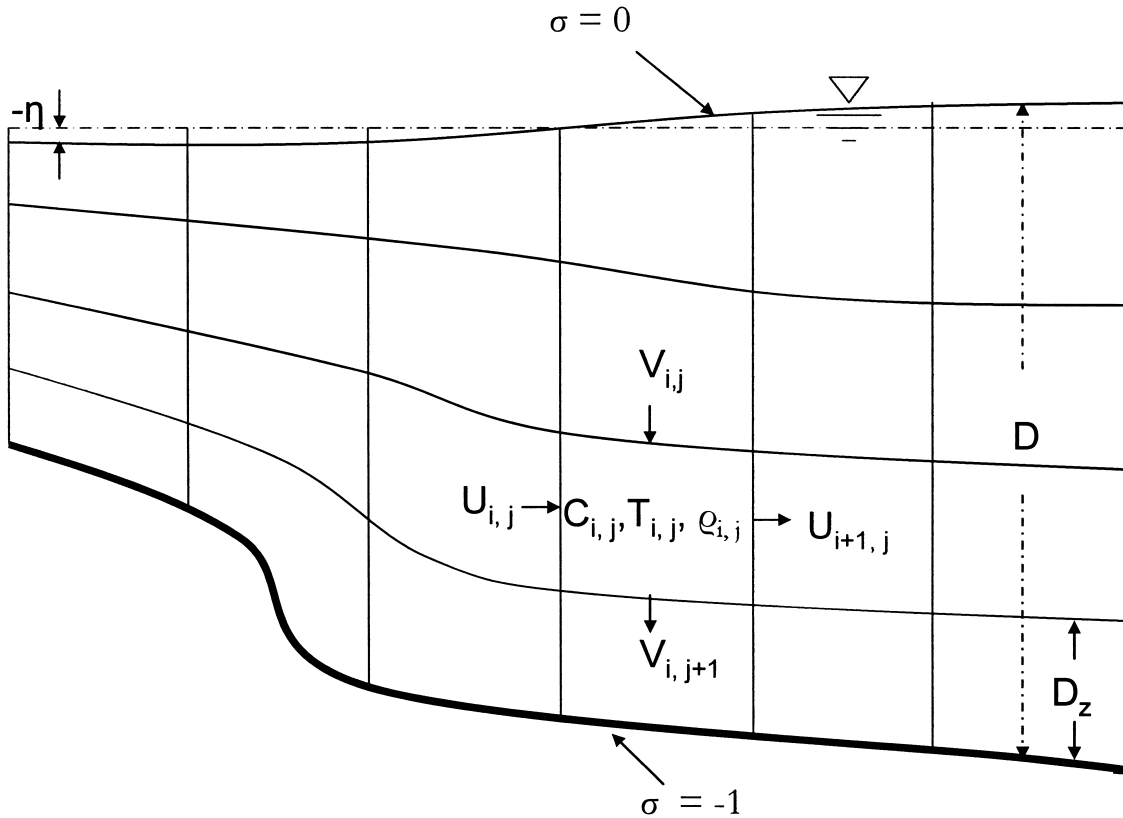


FIG. 2. Sigma layer coordinate system with staggered grids.

where U = longitudinal velocity; V = vertical velocity; P = pressure; ρ = water density; W = river width, ν_x = viscosity in the longitudinal direction and ν_z = viscosity in vertical direction. Assuming hydrostatic pressure, eqn. (1) is solved for U . Continuity is then used to find vertical velocities,

$$\frac{\partial U}{\partial x} + \frac{\partial V}{\partial z} = q_{in} \quad (2)$$

where q_{in} = net lateral inflow per unit volume of each grid cell. It should be noted in the derivation of eqn. (2) that terms involving gradients of width have been neglected.

The surface elevation of the river at the downstream boundary is assumed to be sinusoidal and depends on the amplitude and period of the lake seiche. The water elevation in the entire section of the river is assumed to vary linearly from the downstream boundary (water depth is fixed at the upstream boundary). Thus, the model has a semi-rigid lid and is not able to simulate surface waves, for instance. However, this approach was found to provide stability and to reduce the required

computational time that would have been needed to solve a full free surface formulation. In addition, the main goal of the study did not require detailed hydrodynamic calculations, nor were data available to verify the model, so this simplification was appropriate.

Initial horizontal (longitudinal) velocities are calculated by assuming a logarithmic velocity profile (Jaligama 2004),

$$U = \frac{Q_R}{W z_0} \left(1 + \frac{D}{z_0} \left\{ \ln \left[\frac{D}{z_0} \right] - 1 \right\} \right)^{-1} \ln \left(\frac{D-z}{z_0} \right) \quad (3)$$

where D = depth of the river section; z = depth of the grid element from the surface; and z_0 = height from the bottom of the river where the velocity is zero (i.e., the virtual origin of the profile). The initial vertical velocities in the bottom layer are assumed to be zero and the initial vertical velocities in the other layers are obtained by using the initial horizontal velocities and solving the continuity eqn. (2). (Note that all vertical velocities would be zero initially for a river of constant depth.)

Thermal Stratification (Temperature Balance)

Temperatures in different sections of the river are calculated using a heat balance equation,

$$\frac{\partial T}{\partial t} + U \frac{\partial T}{\partial x} + V \frac{\partial T}{\partial z} = \frac{\partial}{\partial x} \left(k_x \frac{\partial T}{\partial x} \right) + \frac{\partial}{\partial z} \left(k_z \frac{\partial T}{\partial z} \right) - \frac{1}{\rho c} \frac{d\Phi_s}{dz} \quad (4)$$

where T = temperature ($^{\circ}\text{C}$); c = specific heat; Φ_s = solar radiation; and k_x and k_z are thermal diffusivities in the longitudinal and vertical directions, respectively. The solar source term is calculated using a simple exponential decay,

$$\Phi_s = \Phi_{s0}(1 - \beta)\exp(-\eta z) \quad (5)$$

where Φ_{s0} = solar radiation at the surface; β = fraction of radiation absorbed at the surface; and η = absorption or extinction coefficient.

The density of water depends on its temperature and salinity. Since the model is developed for fresh water systems, salinity is neglected and density is obtained by solving the equation of state (e.g., Rubin and Atkinson 2001),

$$\rho = \rho_0 - 0.00663(T - 4)^2 \quad (6)$$

where ρ_0 is the density of water at 4°C ($= 999.97 \text{ kg m}^{-3}$).

Water Quality Model

The water quality model uses mass conservation in the form of an advection-diffusion equation for evaluating the concentrations of CBOD, NH_3 , NO_3 , TON, and DO,

$$\frac{\partial C}{\partial t} + U \frac{\partial C}{\partial x} + V \frac{\partial C}{\partial z} = \frac{\partial}{\partial x} \left(D_x \frac{\partial C}{\partial x} \right) + \frac{\partial}{\partial z} \left(D_z \frac{\partial C}{\partial z} \right) + S_K + S \quad (7)$$

where C = concentration; D_x , and D_z are the longitudinal and vertical diffusivities, respectively; S_K = total kinetic transformation rate; and S = source or sink, where a positive value indicates a source and a negative value indicates a sink. Assuming the diffusivities are driven by turbulent mixing, all diffusivities and viscosities are assumed to take the same values, i.e., $v_x = k_x = D_x$ and $v_z = k_z = D_z$.

The mass balance for DO is dependent not only on the processes affecting it directly, but also on the

processes affecting the other chemical constituents simulated with the model as shown in Figure 3. All the constituents are affected by temperature, external loads, and meteorological conditions, and are transported by advection and diffusion processes. The transformation rates (S_K terms) for the various constituents are described in the following paragraphs.

CBOD

CBOD in the water column is present in both particulate and dissolved forms. The rate of CBOD lost through decay is calculated as a first-order reaction (Wool *et al.* 2003),

$$S_{KCBOD} = -K_b \left(\frac{C_{DO}}{K_{BOD} + C_{DO}} \right) C_{CBOD} - \frac{v_{SBOD}(1 - f_{CBOD})C_{CBOD}}{D} \quad (8)$$

$$K_b = K_{20}[\theta_{CBOD}]^{(T-20)} \quad (9)$$

where K_b = deoxygenation rate coefficient that varies with temperature; K_{20} = rate at 20°C ; v_{SBOD} = CBOD settling rate; $(1 - f_{CBOD})$ = fraction of CBOD associated with settling solids; and θ_{CBOD} = temperature coefficient for CBOD reaction term. The first term in parentheses in eqn. (8) describes the decline in aerobic decomposition of CBOD when the dissolved oxygen concentration in the system is very low and the second term represents a sink for CBOD due to settling. Equation (9) shows the variation in the decay rate as a function of temperature.

Total Organic Nitrogen (TON)

Conversion of TON to ammonia follows a first order reaction (Wool *et al.* 2003),

$$S_{KTON} = -K_{mon}[\theta_{TON}]^{T-20} C_{TON} - \frac{v_{STON}(1 - f_{TON})C_{TON}}{D} \quad (10)$$

where K_{mon} = organic nitrogen mineralization rate at 20°C ; θ_{TON} = temperature coefficient for organic nitrogen mineralization reaction; f_{TON} = dissolved fraction of TON; v_{STON} = TON settling rate; and C_{TON} = concentration of total organic nitrogen. Similar to CBOD, the first term in eqn. (10) represents the loss of TON due to mineralization and the second term represents loss due to settling.

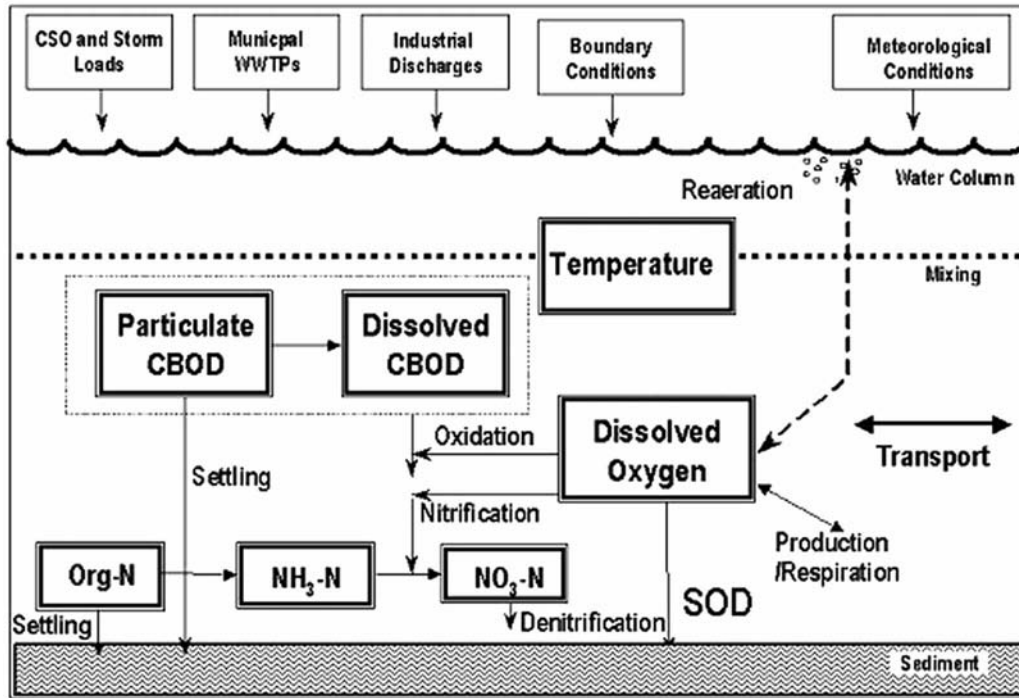


FIG. 3. Processes affecting DO concentration in the water column.

Ammonia (NH_3)

The mineralization of TON (eqn. 10) serves as a source of ammonia, which is also lost from the system through the process of nitrification, in which ammonia is converted to nitrate. The mathematical expression of these processes is given by Wool *et al.* (2003),

$$S_{K_{NH_3}} = K_{mon} [\theta_{TON}]^{T-20} C_{TON} - K_n [\theta_{NH_3}]^{T-20} \left(\frac{C_{DO}}{K_{NIT} + C_{DO}} \right) C_{NH_3} \quad (11)$$

where K_n = nitrification rate at 20°C; K_{NIT} = half saturation constant for oxygen limitation of nitrification; θ_{NH_3} = temperature coefficient for nitrification reaction; and C_{NH_3} = ammonia concentration.

Nitrate (NO_3)

Nitrate is produced by the nitrification of ammonia and is lost from the system through denitrification, by which nitrate is reduced to nitrogen gas under anaerobic conditions. Both of these reactions follow Monod kinetics (Wool *et al.* 2003),

$$S_{K_{NO_3}} = K_n [\theta_{NH_3}]^{T-20} \left(\frac{C_{DO}}{K_{NIT} + C_{DO}} \right) C_{NH_3} - K_{2D} [\theta_{NO_3}]^{T-20} \left(\frac{K_{NO_3}}{K_{NO_3} + C_{DO}} \right) C_{NO_3} \quad (12)$$

where K_{2D} = denitrification rate at 20°C; θ_{NO_3} = temperature coefficient for denitrification reaction; and K_{NO_3} = half-saturation constant for denitrification.

Dissolved Oxygen (DO)

The decomposition (i.e., decay of CBOD) and nitrification losses of DO are calculated as (Wool *et al.* 2003),

$$S_{K_{DO}} = K_b C_{DO} - \left(\frac{64}{14} \right) K_n [\theta_{NH_3}]^{T-20} \left(\frac{C_{DO}}{K_{NIT} + C_{DO}} \right) C_{NH_3} \quad (13)$$

The factor (64/14) in the second term is a stoichiometric ratio, which represents the mass of oxygen consumed per mass of ammonia nitrogen oxidized.

Photosynthesis and Respiration

Phytoplankton concentrations (represented by chlorophyll *a*) were used to estimate the gain and loss of oxygen due to the growth and death, respectively, of phytoplankton (Thomann and Mueller 1987). The gain and loss of DO by photosynthesis and respiration, respectively, can be calculated as (Chapra 1997),

$$Pa = [a_{op} G_{max} (1.066)^{T-20} P] F(I_a) \quad (14)$$

$$R = a_{op} (0.1)(1.08)^{T-20} P \quad (15)$$

where Pa = average gross production; a_{op} = DO/chlorophyll *a* ($\text{mg} \cdot \mu\text{g}^{-1}$); G_{max} = maximum growth rate of phytoplankton; P = chlorophyll *a* concentration; $F(I_a)$ = light attenuation factor; and R = respiration rate. In the model, photosynthesis and respiration rates were computed for optimum or "saturated" light conditions.

Other processes such as SOD and reaeration can be considered as boundary conditions in the model, where SOD is evaluated at the bottom of the water column and reaeration is evaluated at the water surface.

Sediment Oxygen Demand (SOD)

Although SOD serves as a boundary condition, it was convenient to incorporate it as an internal sink in the model, applied to the bottom layer. It is a function of temperature and is calculated as (Thomann and Mueller 1987)

$$S_{BDO} = -\frac{SOD_b}{D_{zbl}} [\theta_{SOD}]^{(T-20)} \quad (16)$$

where SOD_b is the base SOD, for which it is assumed that an adequate supply of oxygen is available in the water column and the temperature is 20°C, θ_{SOD} is the temperature correction coefficient for SOD, and D_{zbl} is the thickness of the bottom water column segment, which is determined internally in the model based on the number of sigma layers and the total depth (this thickness ranges between about 0.15 and 1 m). The variation of SOD due to variations in DO levels is given by Thomann and Mueller (1987) as,

$$SOD = SOD_b \left(\frac{C_{DO}}{K_{SO} + C_{DO}} \right) \quad (17)$$

where K_{SO} = half saturation constant representing the dependence of SOD on DO concentration. Expressing SOD in this way prevents calculations of negative C_{DO} values, which can occur when SOD is specified as a zero-order, or constant sink term.

Reaeration

Atmospheric reaeration is the primary source of oxygen to surface water. The rate of mass transfer of oxygen at the air water interface is directly proportional to the oxygen deficit within the water body,

$$S_{RDO} = a_k (C_s - C_{DO}) \quad (18)$$

where C_{DO} = dissolved oxygen concentration; a_k = reaeration coefficient; and C_s = saturation concentration of dissolved oxygen in the water column. In eqn. (18), the gradient in oxygen concentration is evaluated at the surface, and the reaeration coefficient is calculated as a function of velocity and depth using the O'Connor Dobbins formula (Chapra 1997):

$$a_k = 12.9 v^{0.5} D^{-1.5} \quad (19)$$

where v = average velocity. Although the use of this formula has been questioned for stratified conditions (Atkinson *et al.* 1995), suitable alternatives for such conditions have not been formulated and it was assumed that eqn. (19) would provide reasonable values here.

The saturation concentration of dissolved oxygen is dependent on temperature and is calculated using (APHA 1992)

$$C_s = \exp \left(-139.3441 + \frac{1.5755 \times 10^5}{T_a} - \frac{6.6423 \times 10^7}{T_a^2} + \frac{1.2438 \times 10^{10}}{T_a^3} - \frac{8.62195 \times 10^{11}}{T_a^4} \right) \quad (20)$$

where T_a is absolute temperature (K) of the water at the surface.

Point Sources

Point sources (industrial discharges and discharges from wastewater treatment plants) are incorporated into the mass balance of each constituent (S in eqn. 7). Point sources are modeled

by performing a mass balance for a specified discharge rate on the element closest to the point source location,

$$C = C_0 + \frac{(C_n - C_0)Q_n \Delta t}{\nabla} \quad (21)$$

where C = concentration of constituent (i.e., state variable) being modeled; C_0 = concentration of constituent in the river; Q_n = discharge rate from the point source; C_n = discharge concentration; and ∇ = volume of the element. It is assumed that the mass flux is instantly mixed within the volume of the element into which the discharge occurs. Possible increases in vertical mixing due to the discharges are neglected.

Boundary and Initial Conditions

Boundary conditions for the hydrodynamic model are specified in terms of water depth and flow rate upstream, and water depth downstream. For the vertical and horizontal velocities at the downstream boundary, zero-gradient conditions are assumed. Vertical velocities are zero along the bottom and are equal to the rate of water level changes at the surface. For longitudinal velocities, zero-gradient in the vertical direction is used at the surface and a no-slip condition is imposed at the bottom. The boundary conditions for the water quality model are specified as concentration (or temperature) values both at the upstream and downstream locations. For DO calculations, the surface boundary condition is specified as flux, according to reaeration, and the bottom boundary condition is set to zero flux (SOD is incorporated as an internal sink in the bottom layer—see equations 16 and 17). The upper boundary condition for temperature is determined by surface heat flux, which depends on meteorological conditions and surface temperatures, and zero vertical gradient is set at the bottom. Zero vertical gradients at both upper and lower boundaries are assumed for other water quality constituents.

Initial conditions for all state variables are specified at a number of locations, depending on available measurements, and the model interpolates (or extrapolates) to define values for all numerical grid points. The exception to this is with the initial longitudinal velocities, which are determined by assuming a logarithmic velocity profile (eqn. 3).

MODEL APPLICATION

The model was developed for the Black River, which is a tributary of Lake Erie located near Lorain, Ohio (Fig. 4). It suffers from low DO concentrations, even though significant investments have been made for advanced treatment of waste discharges into the river (Ohio EPA 1999). The river is periodically dredged by the United States Army Corps of Engineers (USACE) for navigational purposes. The dredged section of the river extends from the mouth of the river upstream about 2.8 miles.

The study area extends from the mouth of the river to 4.94 miles upstream (downstream of the confluence of French Creek), as shown in Figure 4. This section of the river receives discharges from outfalls of Republic Technologies International (RTI), the wastewater treatment plant (WWTP) for the City of Lorain (located near the mouth of the river), surface runoff from the sub-watersheds (1 and 2) that drain to this section of the river, and sanitary sewer overflows (SSOs). RTI withdraws water for non-contact cooling and returns the water to the river. The river also receives flows and loads from the Elyria Wastewater Pollution Control Plant (WPCP), the French Creek WWTP (operated by the City of North Ridgeville, OH), French Creek, and significant agricultural loads from the East and West Branches (not shown in Fig. 4) of the Black River.

Bathymetric data for the Black River were obtained from the HEC-2 model input file prepared for the Federal Emergency Management Agency's Flood Insurance Studies (FEMA 1992). Figure 5 shows a depth profile of the model application domain. The depth varies between 1.5 m and 9.8 m and width ranges from 29 m to 220 m.

For this application, the model used 500 segments – 50 segments in the longitudinal direction, and 10 vertical layers with depth of each layer varying between about 0.15 m and 1.0 m. Monitoring of the water quality parameters in the river was conducted in the summer of 2001 on a long-term (bi-weekly for 5 months from May to September) and a short-term (two 5-day intensive survey periods from 25 to 29 June and from 6 to 10 August) basis at various locations (refer to Fig. 5 for station locations). Data were collected by Ohio EPA and contractors for the Black River Cooperative Parties, who funded the study. This monitoring provided large datasets for developing and evaluating the model performance (LTI 2001).

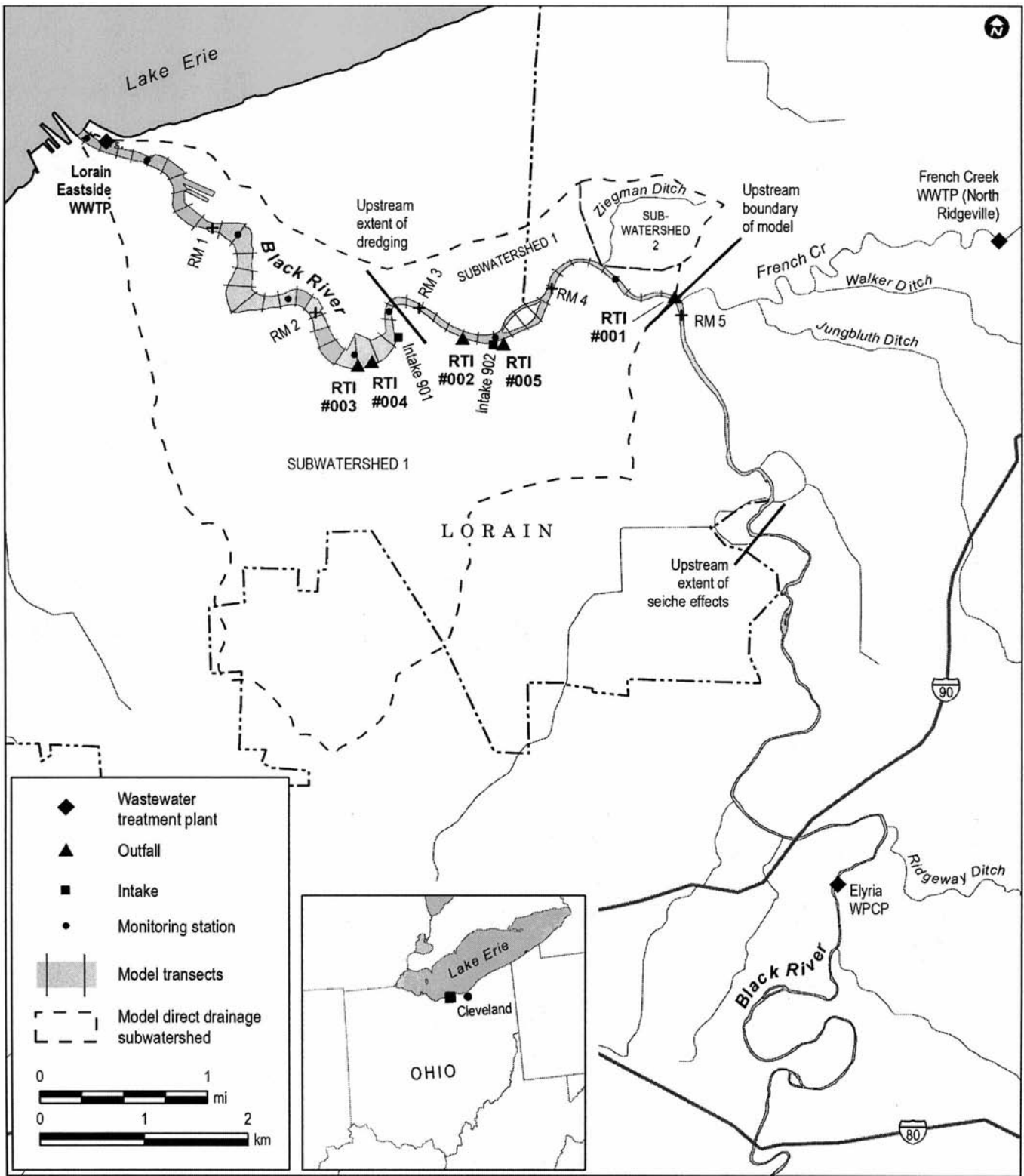


FIG. 4. Model application domain of the lower portion of the Black River with its sub-watersheds, and locations of RTI outfalls, intakes, and the Lorain WWTP.

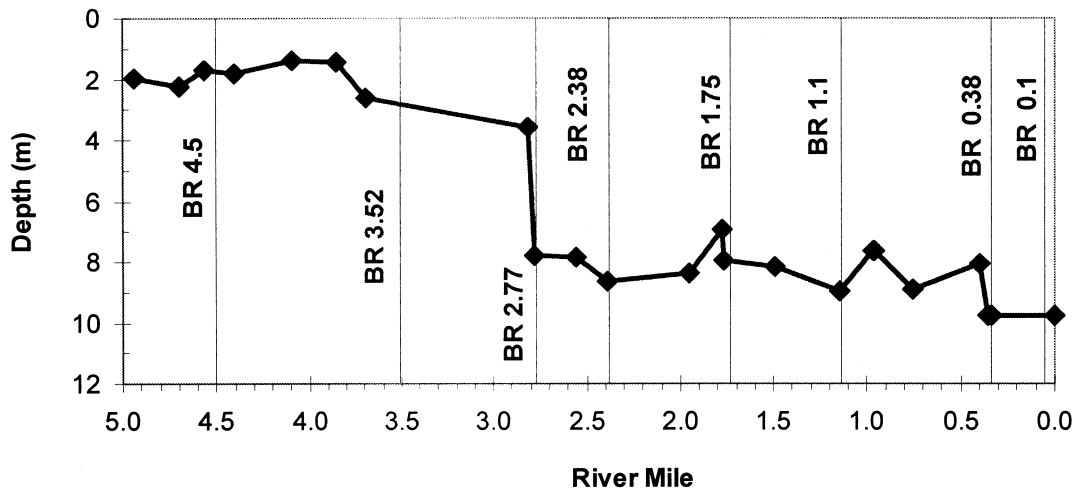


FIG. 5. Depth profile of the model application domain. Vertical lines represent location of 2001 monitoring stations of the Black River (BR).

Hourly average gross flows (without seiche effect) were specified at the upstream boundary at River Mile (RM) 4.94 (7,950 m). The gross upstream flow is the sum of flow recorded at the USGS gage at Cascade Park near Elyria (~RM 15.6—not shown in Fig. 6), flows from the Elyria WPCP, French Creek (including the French Creek WWTP and nonpoint source runoff), surface runoff from nonpoint sources located upstream of the model boundary, and RTI #001. The upstream flow time series, showing the contribution of the different sources from the upper river, is shown in Figure 6. The total flow at this location ranged from $0.5 \text{ m}^3 \text{ s}^{-1}$ to $43 \text{ m}^3 \text{ s}^{-1}$ during the 1 May through 5 September 2001 monitoring period. The significance of the nonpoint sources and the point sources on total river flows when the upstream flows are low can be seen in Figure 6.

A WASP model (LTI 2003) was used to develop upstream (at RM 4.94) boundary concentrations for CBOD, DO, NH_3 , NO_3 and TON. Table 1 provides a summary of loadings from May through September from various sources.

Based on data from Cleveland Port, a seiche with a period of 14.6 hours and amplitude of 0.15 m was determined to represent typical changes in water elevation at the downstream boundary. Data collected at multiple depths from a station located at RM 0.01 were used to establish the downstream boundary concentrations. For the model layers with no measured data, concentrations were estimated based on the measured concentrations above and below

the layer. Data were linearly interpolated to estimate concentrations for days with no sampling data.

Table 2 provides a summary of the range of flows of point and nonpoint sources to the model compared to the gross upstream flow. Data were used to develop time series of flow and concentrations for RTI and Lorain WWTP effluents (LTI 2001). The concentration of the oxygen-demanding constituents from the RTI effluents is negligible compared to the upstream load and the load from other sources in the model. However, the temperature of RTI's effluents is generally higher than the in-stream temperature and thus, potentially affects the temperature balance and thermal stratification simulated by the model. A summary of temperatures of the RTI outfalls is provided in Table 2.

The Lorain WWTP is the principal point source discharging CBOD and nutrients directly to the lower river. Daily flows from the Lorain WWTP were used in the model. For all constituents, the monthly average values were used on days when no data were available.

Previous investigations by the City of Lorain showed a rainfall event with total precipitation of at least one inch is required to trigger an SSO event. SSO flows were estimated using an empirical relationship (LTI 2003). There were only two events in the 1 May to 5 September 2001 simulation period that had sufficient rainfall to cause an SSO event. Even then, the flows from SSOs were insignificant relative to the other sources discharging to the model domain.

Nonpoint source flows from sub-watersheds 1

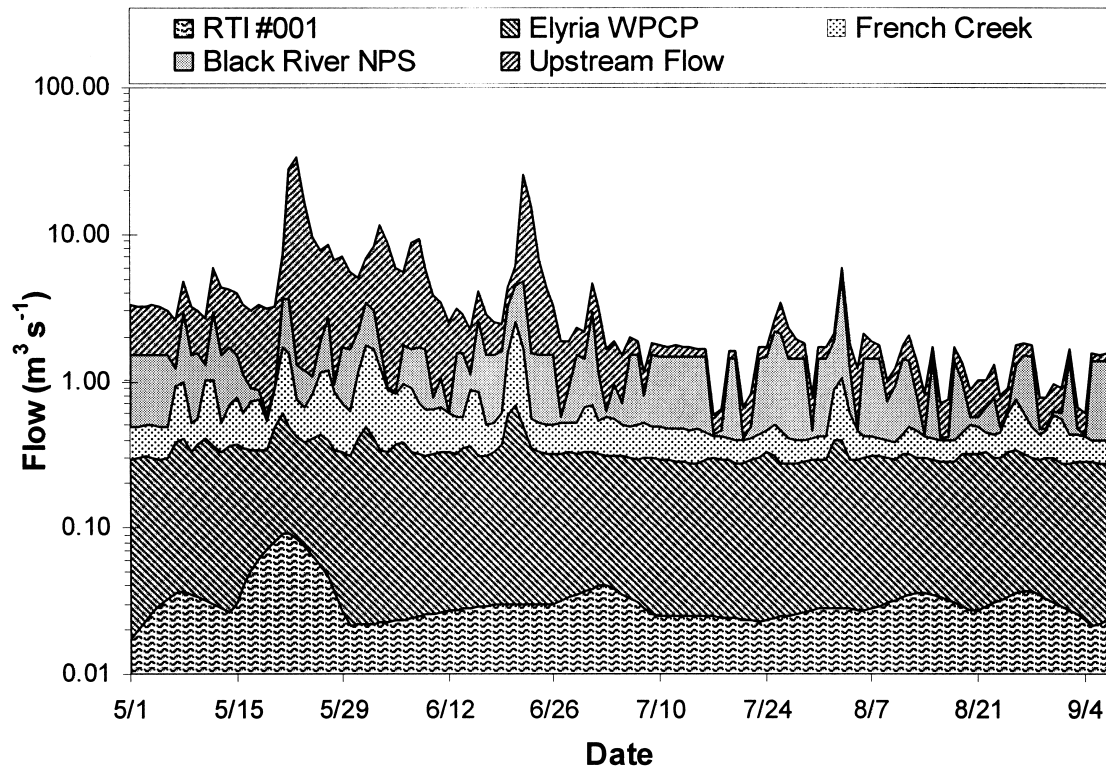


FIG. 6. Time series of upstream river flow, showing contributions from various upstream sources.

and 2 (Fig. 4) that drain to the modeled section of the river were not added to any specific location, but rather were uniformly distributed to the whole channel to reflect the diffuse loading pattern of this source type. A land-use weighted impervious area was multiplied by the precipitation volume of each rainfall event to determine the storm water volume in each sub-watershed. The volume estimated for each sub-watershed was distributed over the duration of the rainfall to develop a flow time series. Event mean concentrations (EMCs) were assigned based on a weighted average pollutant concentra-

tion for different land uses within the sub-watershed. Several sources were used to develop the EMCs, including CERS (2000), Loehr (1974), Novotny (1992, 1991), Jordan *et al.* (2000), and the City of Austin, Texas (1990). The runoff volumes and composite, land use-weighted concentrations from each sub-watershed were then used to calculate the loading time series (LTI 2003).

The pollutant loads from Elyria CSOs were included in the nonpoint source load estimates, and the suitability of representing CSOs in this manner was investigated. Initial values for the SOD base

TABLE 1. Loading summary for the model (from 1 May to 5 September 2001).

Source Type	Volume (MG)	CBOD ₅ Total (kg)	NH ₃ Total (kg)	NO ₃ Total (kg)	TON Total (kg)
Upstream (WASP model output at RM 4.94)	9,915	107,675	5,686	222,654	65,256
NPS (sub-watershed 1)	526	14,621	524	2,643	2,698
NPS (sub-watershed 2)	2	54	2	7	5
Lorain WWTP	1,413	52,440	42,326	12,407	7,233
SSOs	1	47	5	13	10
Total	11,857	174,836	48,543	237,725	75,201

TABLE 2. Range of flows for point and non-point sources to the model (from 1 May to 5 September 2001). Values in parenthesis are the temperatures.

	Flow in m ³ s ⁻¹ (Temperature in °C for RTIs)		
	Minimum	Average	Maximum
Gross US Flow	0.54	3.40	33.40
Sub-watershed 1	0.14	2.17	6.78
Sub-watershed 2	0.001	0.01	0.02
RTI 005	0.30 (18.2)	0.35 (26.8)	0.41 (32)
Intake 902	-0.78	-0.70	-0.64
RTI 002	0.53 (19.9)	0.64 (27.4)	0.74 (34.2)
Intake 901	-3.07	-2.29	-1.40
RTI 004	0.30 (22.6)	0.75 (29.2)	1.81 (34.9)
RTI 003	0.23 (21.8)	1.22 (28.4)	1.90 (34.4)
Lorain WWTP	0.43	0.48	0.83

rates for each model cross-section were estimated from the sediment concentrations of chemical oxidation demand (LTI 2003). The initial estimates of base SOD rates varied between 0.1 and 3.8 g m⁻² day⁻¹ over the model domain. Monthly concentrations for chlorophyll-*a* were used as model input.

MODEL CALIBRATION AND CONFIRMATION

In the calibration process, the site-specific inputs were fixed while the coefficients describing transport kinetics and transformation processes were varied within ranges of values described in the literature (e.g., U.S. EPA 1985). Site-specific inputs include the flows and loads from upstream and various sources within the model domain, cross-sectional areas, boundary concentrations and environmental conditions, such as water temperature. Calibration parameters include the CBOD deoxygenation and settling rates, the nitrification and denitrification rates, the organic nitrogen mineralization and settling rates, and the SOD rates. In general, the calibration proceeded sequentially through the following model constituents:

Temperature → CBOD → Nitrogen species → DO

Following this calibration procedure, the diffusivities were calibrated first using the temperature profiles. As noted above, all diffusivities (for each direction) for each state variable were assumed to

TABLE 3. Kinetic coefficients and transformation rates after calibration.

Description	Symbol	Value	Units	Range	Source
CBOD deoxygenation rate at 20°C	K_b	0.2	day ⁻¹	0.1–0.4	1
½ saturation constant for O ₂ limitation of CBOD	K_{BOD}	0.5	mgO ₂ L ⁻¹		2
Temperature coefficient for CBOD reaction term	θ_{CBOD}	1.056			
Organic nitrogen mineralization rate at 20°C	K_{mon}	0.06	day ⁻¹	0.001–0.4	1
Ammonia nitrification rate at 20°C	K_n	0.2	day ⁻¹	0.009–0.2	1
half-saturation constant for O ₂ limitation of nitrification	K_{NIT}	2.0	mgO ₂ L ⁻¹	0.5–2.0	1
Temperature coefficient for conversion of TON to NH ₃	θ_{TON}	1.07			
Denitrification rate at 20°C	K_{2D}	0.2	day ⁻¹		1
Temperature coefficient for nitrification reaction	θ_{NH3}	1.07			
Temperature coefficient for SOD reaction	θ_{SOD}	1.07			
half-saturation constant for O ₂ limitation for denitrification	K_{NO3}	0.1	mgO ₂ L ⁻¹		2
half-saturation constant for O ₂ limitation on SOD	K_{SO}	2.0	mgO ₂ L ⁻¹		1
TON settling rate	n_{STON}	1.0	m day ⁻¹		
CBOD settling rate	n_{SBOD}	1.0	m day ⁻¹		
Longitudinal diffusivity	k_x, D_x	10 ⁵	cm ² s ⁻¹	10 ⁵ –10 ⁷	3
Vertical diffusivity for surface layer*	k_z, D_z	10	cm ² s ⁻¹	10 ⁻¹ –10 ⁴	3
Vertical diffusivity for deep layers*	k_z, D_z	0.8	cm ² s ⁻¹	10 ⁻² –1	3
Absorption or extinction coefficient	η	1.0	m ⁻¹		
Faction of radiation absorbed at the surface	β	0.4			

*The vertical diffusivity was reduced by 50 percent whenever there is more than 1 deg C difference in temperature between adjacent vertical layers. This is to account for vertical temperature gradients that can reduce vertical mixing.

Source:

1: U.S. EPA 1985

2: Ambrose *et al.* 1993

3: Chapra, S.C. 1997

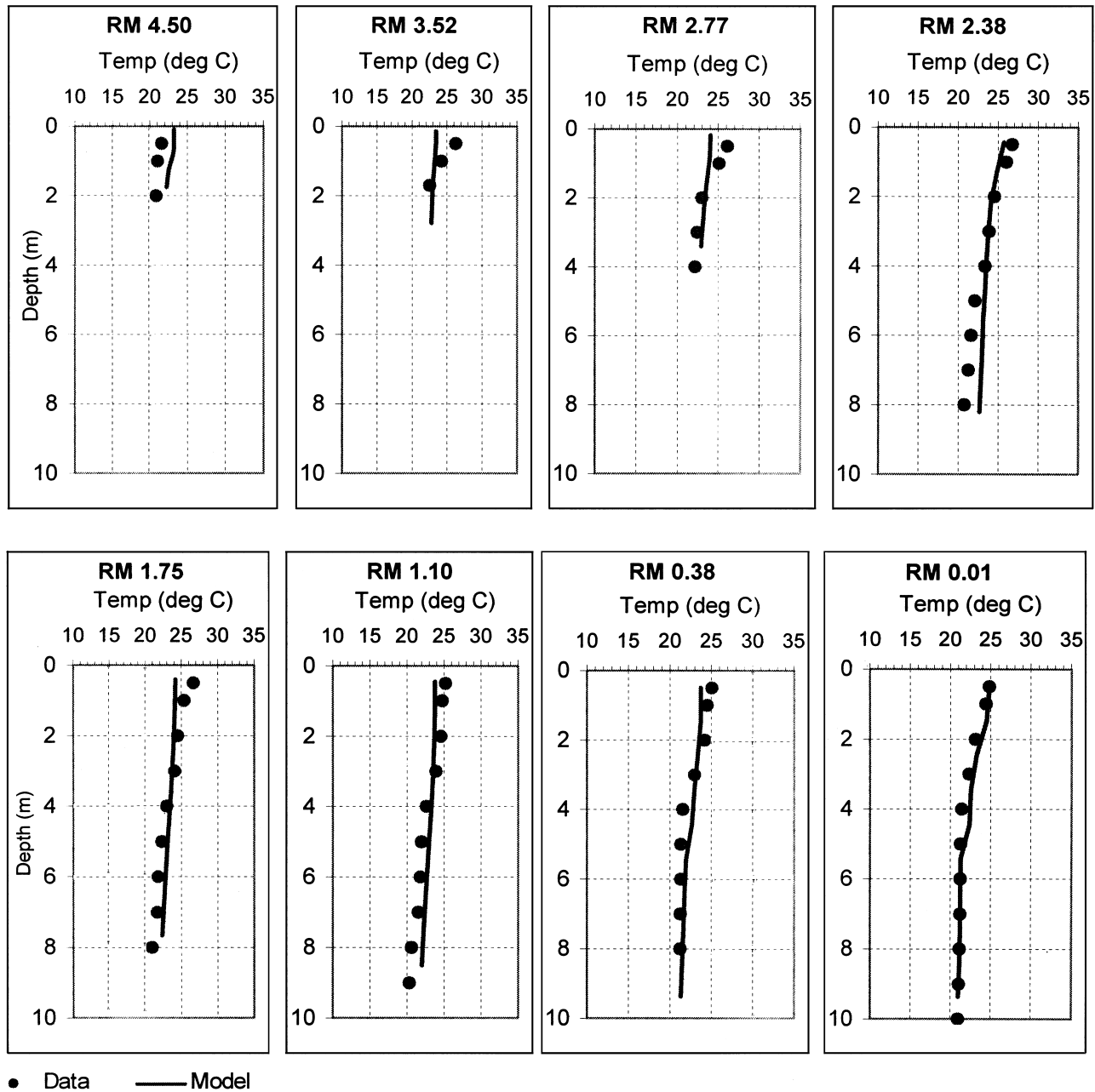


FIG. 7. Model calibration results: depth profiles of temperature showing comparison of model output (line) and measured values (filled circles) at different monitoring locations for 25 June 2001.

take the same value. Also, once calibrated values were determined they were fixed, i.e., they were not calculated as a function of flow, wind, or other conditions. The available data set was not sufficient to develop a detailed model for diffusivities, and the values found here may be considered as average values applicable for the calibration period. Given the model's ability to simulate conditions different

from those for which it was calibrated (the confirmation step, see below), it was concluded that the mixing coefficients determined in this process were adequate for the present study. Once diffusivities were determined, the reaction rates for CBOD and nitrogenous nutrients were calibrated for corresponding concentrations of CBOD, TON, ammonia, and nitrates and nitrites. Once all the rates were es-

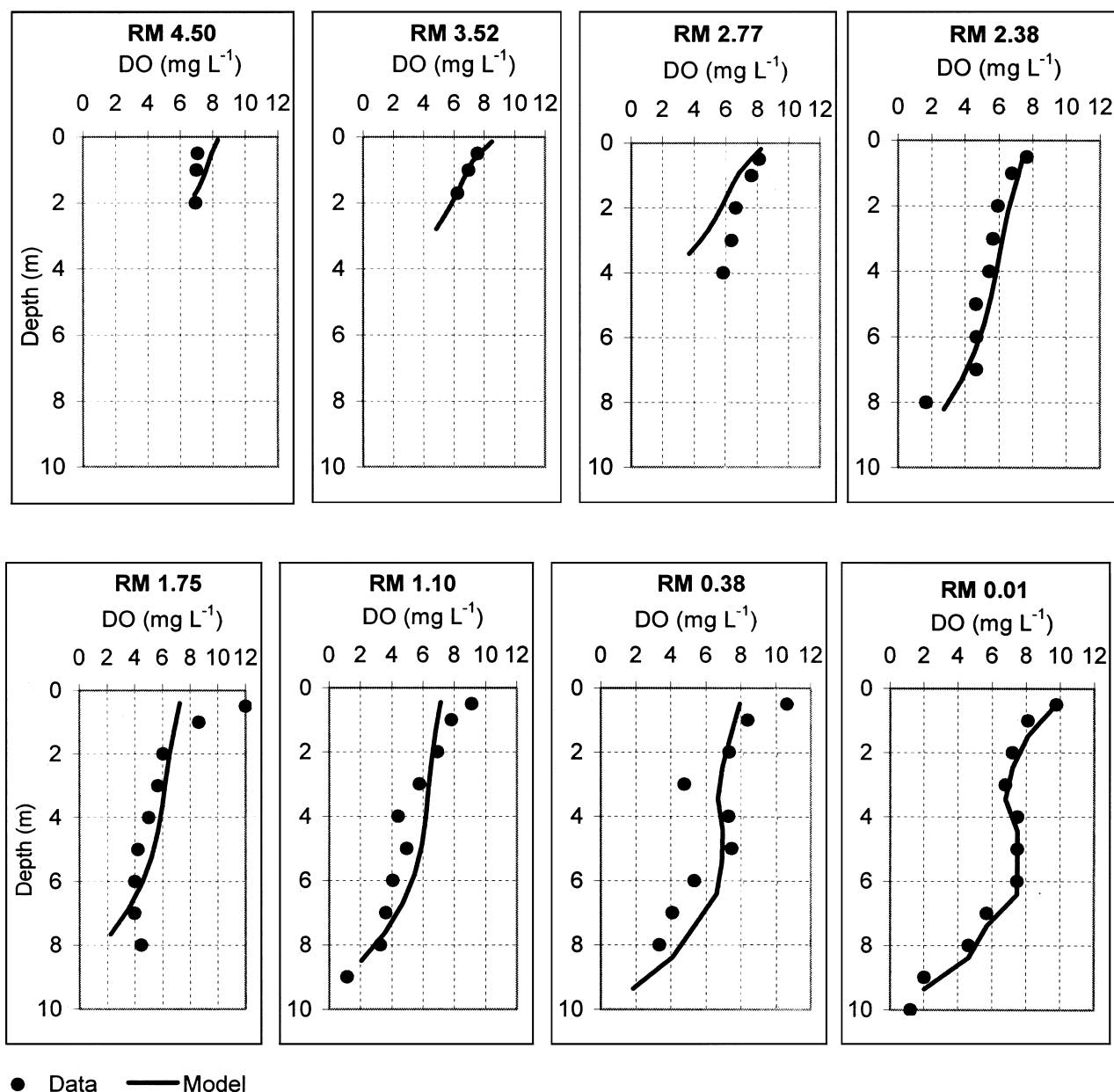


FIG. 8. Model calibration results: depth profiles of dissolved oxygen showing comparison of model output (line) and measured values (filled circles) at different monitoring locations for 25 June 2001.

tablished, the SOD rates were calibrated for DO profiles at the bottom and photosynthesis and respiration rates were adjusted for DO concentrations at the surface.

Following the procedure described above, the model was calibrated for June 2001, with particular emphasis on the 5-day survey (25 to 29 June) for the Black River. Table 3 summarizes the kinetic coefficients and transformation rates obtained after

the calibration process, along with the respective ranges described in the literature.

A comparison of model output and measured values for temperature at different monitoring locations for the Black River for 25 June 2001 is shown in Figure 7. The calibration of temperature is dependent primarily on physical processes such as longitudinal and vertical mixing rates. These rates produced the surface water temperatures as well as

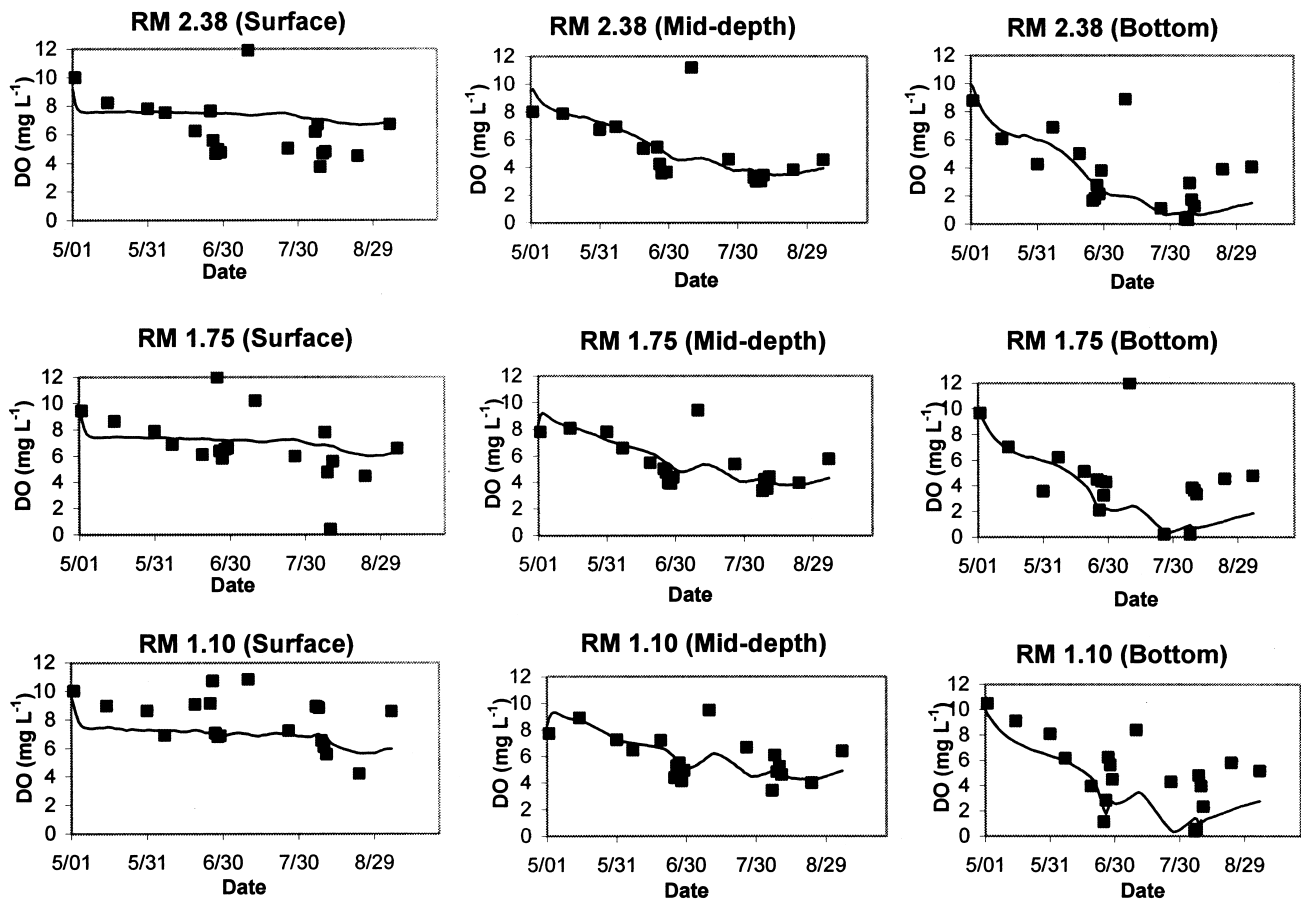


FIG. 9. Model confirmation results: temporal variation in DO showing comparison of model output (line) and measured values (filled rectangles) for surface, mid-depth, and bottom layers at RMs 2.38, 1.75, and 1.10.

the vertical gradients of decreasing temperature with depth in the navigational channel reasonably well (see below for further discussion of model fit). Surface temperatures during the period never exceeded 30°C.

A depth-wise comparison of the model output and the measured values for the DO concentrations at different monitoring locations for 25 June 2001 is shown in Figure 8. Dissolved oxygen profiles generated by the model compare well with observations, particularly in the lower layers of the channel reach between RM 2.38 and the river mouth. The DO standard is violated in this reach as shown by both the model and the data. Good agreement between the model results and data for CBOD, NH₃, and NO₃ were also obtained (Jaligama 2004).

The model confirmation results for DO concentrations in the surface, middle and bottom layers at

RM 2.38 (the location where the depth and width changes drastically) and at RM 1.75 and 1.10 from May to September 2001 are shown in Figure 9. This comparison demonstrates that the model captures the time trends in DO quite well. The DO in the bottom layers goes below 4 mg L⁻¹ starting from mid-June to the end of the summer, even reaching below 1 mg L⁻¹ at several locations.

To better quantify the degree to which the model fits measured data, cumulative frequency distributions for all model results are shown for temperature and DO in Figures 10 and 11, respectively. These paired comparisons between the model results and data were based on the two weekly extensive sampling periods (25–29 June 2001 and 6–10 August 2001). Data collected at all sampling locations and at various depths were used for conducting this analysis.

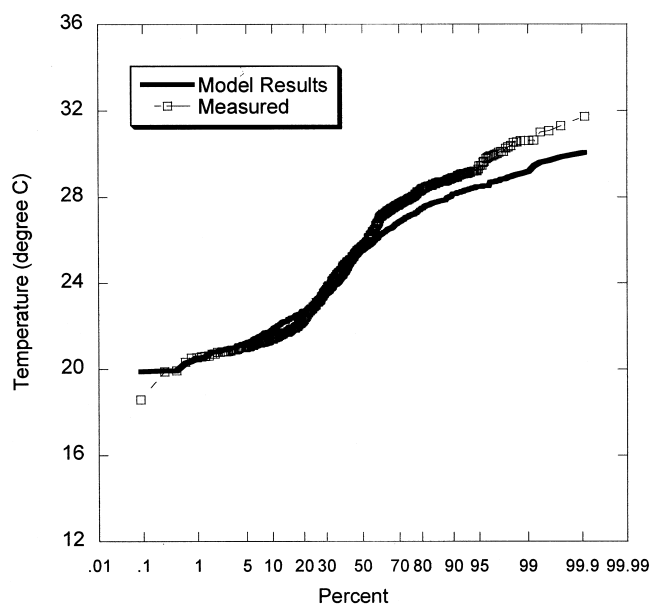


FIG. 10. Cumulative frequency distribution plot showing the comparison between the model-simulated and measured temperature at all sampling locations monitored during the two extensive monitoring periods (25 to 29 June 2001 and 6 to 10 August 2001).

As presented in Figure 10, the model results compare well with measured data below 26°C. However, the model under predicted the measured temperatures near the water surface (higher values). Note that the surface temperature data were collected at the water surface, whereas the model results represent water temperature at some depth below the surface, depending on grid thickness, so that a slight under-prediction of surface temperature is to be expected.

As seen in Figure 11, the model under predicted DO concentrations for values above 10 mg L⁻¹, which represents the near surface conditions. It is believed that the DO concentrations at the water surface were not simulated properly because chlorophyll *a* data were not available for all stations at all times. No attempt was made to better represent the high DO values (at the surface) with the model since the main concern for this study was for lower concentrations. In addition, it is to be noted that the data and the model results do not always correspond spatially to each other. For example, the data were collected at a particular depth in the water column, whereas a model result repre-

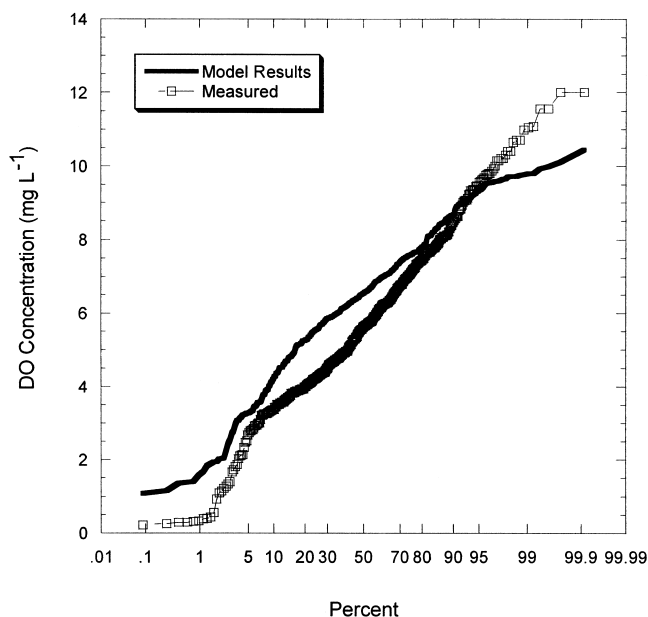


FIG. 11. Cumulative frequency distribution plot showing the comparison between the model-simulated and measured dissolved oxygen concentrations at all sampling locations monitored during the two extensive monitoring periods (25 to 29 June 2001 and 6 to 10 August 2001).

sents a layer of finite thickness, uniform over its depth.

It should also be noted that the model tends to slightly over predict DO values at the lower end, which should be taken into account when estimating possible regulatory actions. However, the main purpose of the present study was to identify causes of low DO, and that result is not affected by the slight over prediction.

Table 4 provides estimates of errors between the model results and data measured during the two weekly sampling periods in 2001 for temperature and DO concentrations. In this table, the “relative error” is simply the average of all differences between the paired measured and simulated values, and “absolute error” is the average of the absolute values of the differences. As can be seen, the root mean square error (RMSE) is largest, since extreme differences, while few in number, are emphasized in the squaring process. The relative and absolute errors, compared with typical magnitudes for temperature and DO, are considered to be within a reasonable range for this application.

TABLE 4. *Statistical measure of the errors between the model-simulated and measured dissolved oxygen concentrations at all sampling locations monitored during the two extensive monitoring periods (25 to 29 June 2001 and 6 to 10 August 2001).*

Parameter	Relative Error	Absolute Error	Root Mean Square Error (RMSE)
Temperature (°C)	-0.39	0.67	0.94
DO (mg L ⁻¹)	0.77	1.24	1.76

DIAGNOSTIC ANALYSIS AND RESULTS

The calibrated and confirmed model was applied in a diagnostic mode to understand the impact of various sources on DO concentrations. The aim of the Black River model application was to understand the factors contributing to low DO in the channel and to evaluate whether DO standards can be attained with technically feasible and economically achievable point and nonpoint source control strategies.

A series of model runs was performed to assess the effects of the WWTP loads, thermal discharges from RTI and the upstream and nonpoint source loads on the DO concentrations. As mentioned earlier, the conditions (i.e., loads, inputs, and results) used in the model confirmation run served as the baseline for the sensitivity analysis. In the reduced loading scenarios, SOD rates were kept constant. However, in reality, reduction in pollutant loads would likely reduce SOD, so that the results presented here are probably conservative in terms of predicting lower DO concentrations than might actually occur.

Zero Point Source Pollutant Loads

To assess the effect of point sources on DO concentrations, the loads of oxygen-demanding constituents (CBOD, DO, NH₃, NO₃, TON) from the Elyria PCP, the N. Ridgeville WWTP, and the Lorain WWTP were set to zero. Two separate model runs were conducted. In the first run, the loads from the Elyria PCP and the N. Ridgeville WWTP were set to zero. A comparison of the DO concentration with the baseline results showed a small (~0.5 mg L⁻¹) increase in DO concentration at RM 2.38 in the middle layer. Almost insignificant changes in the DO concentration were found for the surface and bottom layers. In the second model run, loads from all three WWTPs were set to zero. Compared to the results from the first model run, the second model run showed a maximum increase of 0.5 mg L⁻¹ in surface DO concentration at RM 1.10, while

there were insignificant changes in DO concentration in the middle and bottom layers. The impact seen at RM 1.10 might be caused by the location of the Lorain WWTP. It appears that the impacts of point source discharges on the DO concentration are small and are influenced by the outfall locations of the WWTPs.

Zero Upstream Pollutant Loads

The model was run with zero upstream pollutant loads while keeping the nonpoint source loads and other flows and loads the same as the baseline run. A comparison of DO concentrations with the baseline results for the lower portion of the river showed that the DO concentrations increased slightly (< 0.5 mg L⁻¹) in the middle portions of the river. This suggests that upstream pollutant loads have a small effect on the bottom DO concentration.

Reduced Upstream and Nonpoint Source Pollutant Loads

To assess the effect of upstream and nonpoint source loads, the pollutant concentrations were reduced by half of their baseline values. This change in loads resulted in only about a 0.5 mg L⁻¹ increase in DO in the mid to bottom layers at RM 2.38. This suggests that nonpoint sources are not important.

Increased RTI Discharges

The discharge and temperature concentrations from all the RTI outfalls were increased by 33 percent and the water intakes were also adjusted to account for increased water withdrawals. Model results indicated that the DO concentration was slightly increased in the surface layer, which might be due to the increased withdrawals. The changes in DO concentrations at the mid-depth and lower layers were negligible (Jaligama 2004). RTI discharges have the most effect at the surface at RM 2.38 (near

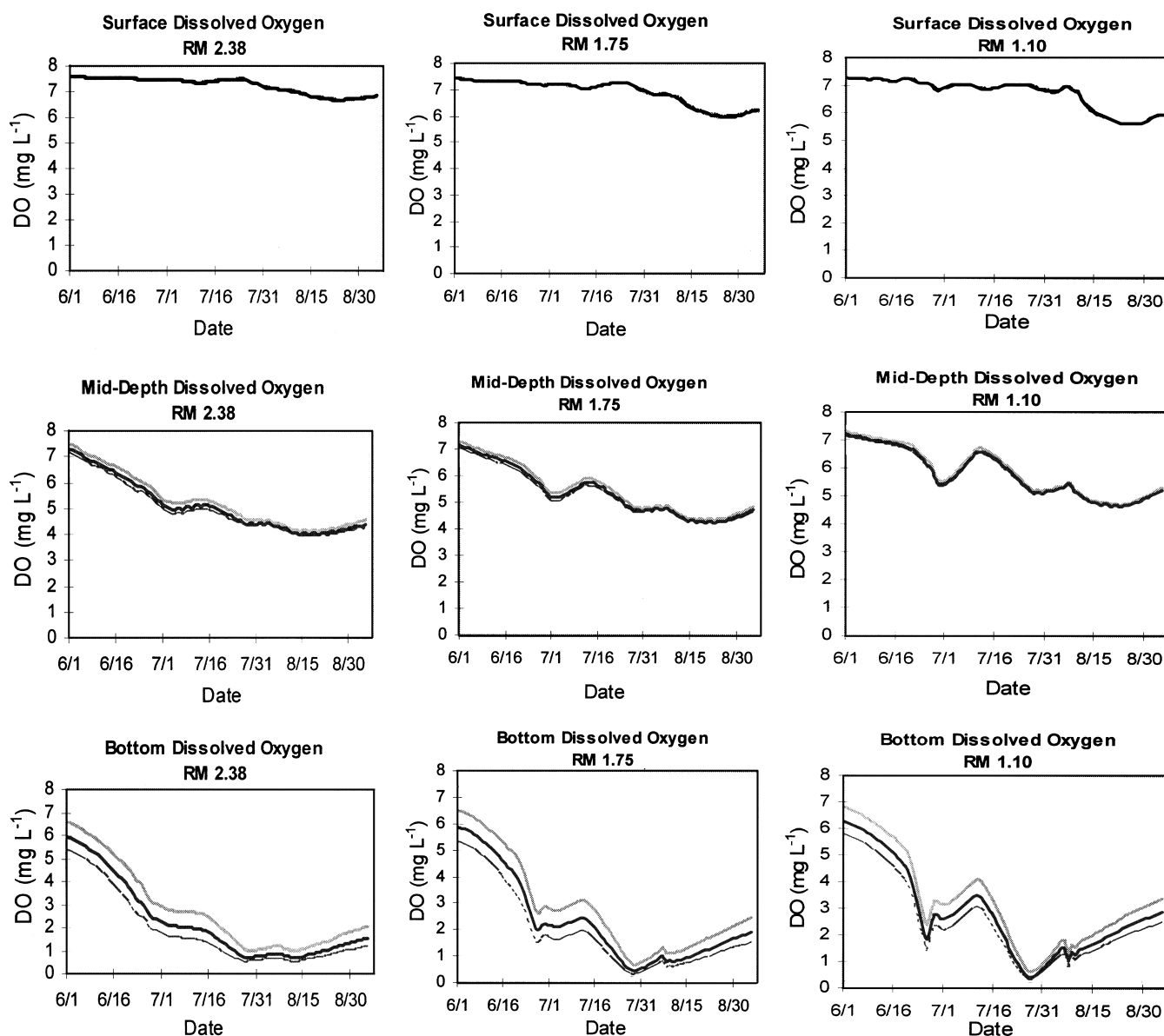


FIG. 12. Comparison of DO profiles for 25 percent increased (line) and 25 percent decreased (light thick line) SOD rates with baseline (dark thick line) results at RMs 2.38, 1.75, and 1.10 for the surface, mid-depth, and bottom layers.

RTI #003). However, the effect of RTI discharges on bottom water temperature is negligible.

Changes in SOD Rates

The base SOD rates were increased and decreased by 25 percent of the baseline values. The maximum changes in DO concentration relative to baseline were 24 percent and 20 percent with 25 percent increase and decrease in SOD rates, respectively,

at the bottom layer at RM 2.38 (Fig. 12). There are also significant responses in DO in the bottom layer at RM 1.75 (21 percent and 18 percent change in DO with 25 percent increase and decrease in SOD rates, respectively) and RM 1.10 (16 percent and 15 percent change in DO with 25 percent increase and decrease in SOD rates, respectively). Differences in DO concentrations at mid-depth are considerably less (0.3-0.5 mg L⁻¹) than in the bottom layer, indicating that stratifica-

tion reduces the influence of SOD on oxygen resources at depths above the bottom. This result also reflects the relatively low vertical mixing rates in the river. Diffusivities were calibrated using temperature data, as previously described, and higher vertical mixing rates would presumably lead to greater mixing of low DO water upward. On the other hand, greater vertical mixing would also enhance the impact of surface aeration, and the net effect of these two processes can be variable. Since mixing similarly affects all chemical species in the model, it is difficult to isolate the effect of vertical mixing on the results, and there was no attempt made to consider model sensitivity to variations in diffusivities. Differences in DO concentrations at the water surface were negligible throughout the simulation period at all locations, and it was concluded that SOD is the primary sensitivity parameter affecting the DO levels at the critical locations of the channel where DO violations have occurred.

DISCUSSION

This work demonstrates the development and application of a coupled two-dimensional, hydrodynamic/water quality model for a dredged river, which typically becomes stratified in summer. Model results showed that the DO concentrations in surface waters of the river are always above 5 mg L⁻¹ and DO violations occur mostly in the bottom layers. The region of low DO starts near the upstream limit of navigational dredging, and it appears that SOD, combined with altered hydraulics due to dredging, is the main cause of DO violations.

Navigational dredging has caused significant changes in physical and hydraulic conditions in the Black River as shown in Figure 1. Moreover, such changes in morphology due to navigational dredging are not unique in the Great Lakes basin. For example, a similar situation is observed with the Buffalo River (Buffalo, New York). Jalgama (2004) applied the model to understand the DO dynamics due to changes in morphology and hydraulics resulting from navigational dredging in the Buffalo River. Similar to the Black River, velocities are strongly affected and mixing is reduced, contributing to the stratification of the river in the late spring and early summer. In both rivers, the thermal stratification combined with the low flows during the summer decreases vertical mixing in the water column and isolates a pocket of water near the bottom that is significantly impacted by SOD while at the same time receiving very limited atmospheric

reaeration. It should be noted that the SOD is determined by deposition of oxygen demanding material to the sediment surface, which changes continuously due to physical-chemical-biological conditions in the river. Flow reversals along the bottom of the channel due to seiches of colder lake water also have the effect of increasing water residence time (LTI 2001), thus allowing SOD to have a larger impact. With prolonged residence times, sometimes lasting up to four or five days (in the Buffalo River case), even with a low SOD there is sufficient time for significant oxygen demand to be exerted. For example, for a residence time of 5 days and SOD as low as 1 g m⁻² d⁻¹ in a bottom layer of 1 m depth, a drop in DO concentration of 5 mg L⁻¹ could occur due to SOD. As found in the present Black River study, the DO results in the Buffalo River application were also found to be most sensitive to the SOD rates. Thus, the impact on DO concentration due to SOD rates in conjunction with the changes in hydraulics of the channel due to navigational dredging as found for the Black River and the Buffalo River is expected to be found in most Great Lakes tributaries that are periodically dredged.

It should be noted that vertical mixing in the stratified zone of the river and SOD interact to either produce large DO concentration sensitivity to SOD in a relatively thin bottom layer of water (low vertical mixing) or to spread out (and thus reduce the DO concentration change) the areal SOD-induced DO concentration response over a thicker bottom layer (higher vertical mixing). So with high vertical mixing, the impact of a given SOD would be spread out over a greater depth, and therefore the concentration effect would be mitigated to some extent.

It should also be noted that navigational dredging may impact SOD due to the removal of oxygen demanding materials. The impact of dredging on the reduction of SOD may occur for a short period of time (i.e., just after the dredging) due to removal of surface sediments yet to undergo diagenetic processes, but oxygen demand would not be eliminated since over time additional oxygen-demanding materials would be continuously deposited.

SUMMARY AND CONCLUSIONS

The coupled 2-dimensional (laterally averaged) hydrodynamic-dissolved oxygen model developed and applied herein has been successful in simulating stratified conditions in the Black River. Furthermore, it has been designed to simulate the effects of

multiple point and nonpoint source discharges, withdrawals from the river, time dependent boundary conditions and changes in the water levels at the downstream boundary. The model produced reasonable results to represent the observed spatial and temporal trends in the dredged portions of the Black River for temperature, CBOD, ammonia, organic nitrogen, nitrate, and DO concentrations. The diagnostic analysis indicated that there are no reasonable point source controls that can increase DO concentrations above 4 mg L^{-1} at all times.

Results from the present application, as well as a similar application to the Buffalo River, support the conclusion that SOD, combined with alterations in flow hydraulics due to navigational dredging, are the main contributors to low DO levels, and it may be expected that similar conditions should prevail for other Great Lakes tributaries. These results give rise to an interesting question: what is the contribution of deposition of organic matter originating from upstream, CSOs, and nonpoint sources on SOD rates? A more detailed assessment of oxygen demanding sediment sources and sinks from upstream and nonpoint sources would be necessary prior to implementing a watershed management plan aimed at reducing SOD in the dredged portion of the rivers.

It should be noted that the model does not include phosphorus dynamics. Addition of the phosphorus cycle would allow the model to predict phytoplankton blooms and their impact on DO concentrations. A more complete picture of relationships among external phosphorus loadings, cycling of phosphorus internally in the system, and its impact on DO dynamics would require extension of the model to incorporate organic and dissolved phosphorus kinetics similar to nitrogen and dissolved oxygen kinetics. This application would require additional site-specific data for these variables.

The model is not capable of handling branched systems. Tributaries to the main stem of the river can be added as point sources, but they cannot be modeled simultaneously with the main stem of the river. Modifications to handle branched systems would make the model applicable to any number of water bodies linked together.

ACKNOWLEDGMENTS

The model development and its application to the Black River were conducted under a contract from the Black River Cooperative Parties to Limno-Tech,

Inc. and sub-contract to the University at Buffalo. The application of the model to the Buffalo River was carried out by the University at Buffalo with a contract from Malcolm-Pirnie. We thank the Cities of Elyria, Lorain and North Ridgeville, OH, and RTI for providing the database necessary for modeling the Black River. The authors also acknowledge the significant contributions of the Ohio EPA staff to the monitoring program. Comments from the reviewers of the first draft of this manuscript are also appreciated.

REFERENCES

- Ambrose, R.B., Jr., Wool, T.A., and Martin, F. 1993. *The water quality analysis simulation program, WASP5, Part A: model documentation*. U.S. Environmental Protection Agency, Athens, GA.
- APHA. 1992. *American Public Health Association, standard methods for the examination of water and wastewater*, 18 ed. Washington DC.
- Atkinson, J.F., Blair, S., Taylor, S. and Ghosh, U. 1995. Surface aeration. *J. Environ. Eng.* 121 (1):113–118.
- Blair, S.H. 1992. Dissolved oxygen modeling for the Buffalo River. M.S. thesis, Dept. Civil, Structural and Environ. Eng., Univ. at Buffalo.
- Brown, L.C., and Barnwell, T.O., Jr. 1987. *The enhanced stream water quality models, Qual-2E and Qual-2E UNCAS: Documentation and users manual*. EPA/600/3-87/007, Environ. Res. Lab., U.S. Environmental Protection Agency, Athens, GA.
- Center for Environmental Research and Service (CERS), 2000. *Characteristics of pollutants in storm water runoff from Dothan, Alabama catchments: Implications for Phase II storm water management*. Prepared for the Alabama Department of Environmental Management.
- Chapra, S. 1997. *Surface water-quality modeling*. New York: McGraw Hill Companies, Inc.
- City of Austin, Texas. 1990. *Stormwater Pollutant Loading Characteristics for Various Land Uses in the Austin Area*. Prepared by the Watershed Protection and Development Review Department. www.ci.austin.tx.us/watershed/rptswload.htm
- Clark, M.M., 1996. *Transport modeling for environmental engineers and scientists*. New York: John Wiley and Sons, Inc.
- Cole T., and Buchak, E. 1995. *CE-QUAL-W2: A two-dimensional, laterally averaged, hydrodynamic and water quality model*. Version 2.0, Tech Rpt. EL-95-May 1995, Waterways Experiments Station, Vicksburg, MS.
- FEMA. 1992. *Flood Insurance Study*. The City of Lorain, Ohio.
- Hall, J. 1997. Dissolved oxygen modeling for the Buffalo River. M. Eng. project, Dept. Civil, Structural and Environ. Eng., Univ. at Buffalo.

- Jaligama, G.K. 2004. A two dimensional coupled hydrodynamic/water quality model for Great Lakes Tributaries. M.S. thesis. Dept. Civil, Structural and Environ. Eng., Univ. at Buffalo.
- Jordan, T.E., Correll, D.L., and Weller, D.E. 2000. *Mattawoman Creek Watershed: Nutrient and Sediment Dynamics*. Smithsonian Environmental Research Center, Edgewater, MD. www.charlescounty.org/pgm/planning/plans/environmental/mattawoman/sercreport.pdf
- Kantha, L.H., and Clayson, C.A. 1994. An improved mixed layer model for geophysical applications. *J. Geophysics. Res.* 99:25235–25266.
- Limno-Tech, Inc. (LTI). 2001. *Design of modeling and monitoring programs for the lower Black River water quality model, Phase I Report. Prepared for the Black River Cooperative Parties. Supplemented with Revised Section 3.4 of the Lower Black River Phase I Report.* Draft. Prepared for the Black River Cooperative Parties.
- . 2003. *Development of a WASP model of the free-flowing portion of the Black River.* Memorandum to the Black River Cooperative Parties.
- Loehr, R.C. 1974. Characteristics and Comparative Magnitude of Non-point Sources. *Journal WPCF* 46(8):1849–1872.
- Novotny, V. 1991. *Urban Diffuse Pollution: Sources and Abatement.* Water Environ. Tech. 3(12):60–65.
- . 1992. *Unit Pollutant Loads: Their Fit in Abatement Strategies.* Water Environ. Tech. 4(1):40–43.
- Ohio EPA. 1999. *Biological and Water Quality Study of the Black River Basin, Lorain and Medina Counties.* State of Ohio Environmental Protection Agency, Columbus, Ohio, March 31, 1999.
- Rubin, H., and Atkinson, J. F. 2001. *Environmental Fluid Mechanics*. New York: Marcel Dekker, Inc.
- Thomann, R.V., and Mueller, J.A. 1987. *Principles of surface water quality modeling and control*. New York: Harper Collins Publishers.
- U.S. Environmental Protection Agency (U.S. EPA). June 1985. *Rates, constants, and kinetics formulations in surface water quality modeling (second edition)*. Environmental Research Laboratory. EPA/600/3-85/040. Athens, GA.
- . 1986. *Ambient water quality criteria for dissolved oxygen*. Criteria and standards division. U.S. Environmental Protection Agency, Washington, D.C. EPA 440/5-86-003.
- Wight, M. 1995. A numerical model to examine dissolved oxygen in the Buffalo River. M. Eng. project. Dept. Civil, Structural and Environ. Eng., Univ. at Buffalo.
- Wool, T.A., Ambrose, R.B., Martin, J.L., and Comer, E.A. 2003. *Water Quality Analysis Simulation Program (WASP6)*. Draft User's manual, version 6. Environmental Research Laboratory, U.S. EPA, Athens, GA (http://www.epa.gov/region4/water/tmdl/tools/WASPG_Manuel.pdf)
- Zhao, P.A. 2002. Analysis of numerical dispersion of 2-D alternating-direction implicit FDTD method IEEE Trans. *Microwave Theory Tech.* 50:2003–2007.

Submitted: 10 December 2005

Accepted: 22 October 2006

Editorial handling: William M. Schertzer